nature chemistry

ARTICLES

PUBLISHED ONLINE: 22 SEPTEMBER 2013 | DOI: 10.1038/NCHEM.1752

A clamp-like biohybrid catalyst for DNA oxidation

Stijn F. M. van Dongen[1†], Joost Clerx[1†], Kasper Nørgaard[1], Tom G. Bloemberg[1,2], Jeroen J. L. M. Cornelissen[1], Michael A. Trakselis[3], Scott W. Nelson[4], Stephen J. Benkovic[5], Alan E. Rowan[1*] and Roeland J. M. Nolte[1*]

In processive catalysis, a catalyst binds to a substrate and remains bound as it performs several consecutive reactions, as exemplified by DNA polymerases. Processivity is essential in nature and is often mediated by a clamp-like structure that physically tethers the catalyst to its (polymeric) template. In the case of the bacteriophage T4 replisome, a dedicated clamp protein acts as a processivity mediator by encircling DNA and subsequently recruiting its polymerase. Here we use this DNA-binding protein to construct a biohybrid catalyst. Conjugation of the clamp protein to a chemical catalyst with sequence-specific oxidation behaviour formed a catalytic clamp that can be loaded onto a DNA plasmid. The catalytic activity of the biohybrid catalyst was visualized using a procedure based on an atomic force microscopy method that detects and spatially locates oxidized sites in DNA. Varying the experimental conditions enabled switching between processive and distributive catalysis and influencing the sliding direction of this rotaxane-like catalyst.

Enzymes that are able to thread onto biopolymers and to perform stepwise reactions along the polymer chain, such as toroidal processive enzymes, are among the most fascinating tools involved in the cellular machinery. Processive catalysis is ubiquitous in nature, whereas non-templated distributive catalysis is the most common mode of operation for both homogeneous and heterogeneous catalysts[1]. Examples of processive catalysts are DNA polymerases and exonucleases, which play crucial roles in numerous events during the life cycle of a cell, including most of the replication, transcription and repair processes[2–7]. Clamp-shaped proteins are central components in these metabolic processes. They encircle DNA and can tether other proteins or enzymes through specific binding interactions. Clamp proteins can track along DNA, either as a single entity or as an enzyme carrier, and are loaded at recognition sites by clamp-loader proteins. Therefore, the clamp enhances the association of its recruited enzyme, which confers processivity to the latter's catalytic action. A well-studied example is the replication system of the bacteriophage T4, which employs a trimeric ring-shaped clamp (gp45) to associate with the replication polymerase (gp43) to DNA, and thereby dramatically enhances the processivity of the latter enzyme[8,9]. Although the clamp itself has no catalytic function, effectively it enables the polymerase to switch from a distributive to a processive mode of action, paramount to the efficiency of the replication process.

In the past, many studies reported on synthetic systems that model the catalytic action of enzymes[10–12]. In contrast, very few efforts were made to mimic the processive properties of these biomacromolecules[13]. In previous papers, we described a synthetic catalyst based on a macrocyclic porphyrin complex that can thread onto a synthetic polymer chain (polybutadiene) and oxidize its double bonds via a hopping mechanism[14–16], and thereby act as a primitive model of a processive enzyme. In the present paper we report on a biohybrid mimic derived from the T4 sliding clamp protein. The mimic is equipped with a porphyrin derivative to yield an artificial enzyme that can oxidize DNA substrates. Depending on the reaction conditions, its mode of catalysis can be influenced from a distributive to a processive mode of action. The oxidation reactions are monitored at the single-molecule level using a novel streptavidin-labelling procedure in combination with atomic force microscopy (AFM), which provides a tool that can not only detect catalytic events, but also spatially relate them to each other. As a catalyst we used the manganese tetramethyl pyridinium porphyrin complex (Mn-TMPyP, **1**, see Fig. 1), which together with an oxygen donor can cleave selectively double-stranded DNA (dsDNA) templates at sequences that contain three consecutive adenosine–thymine (A-T) base pairs[17–19]. The main pathway of this oxidation process entails hydroxylation at the C5′ position of the deoxyribose ring of the DNA backbone, which leads to a nick at the 3′ end of the AAA sequence. This nick contains an aldehyde group at its 5′ end, which forms a suitable target for the above-mentioned streptavidin assay. Combining the activity of this porphyrin with the DNA-tracking behaviour of the T4 clamp protein thus effectively creates a biohybrid catalyst with a processive character.

Results and discussion

Design of the clamp-shaped biohybrid catalyst. A maleimide-functionalized porphyrin based on Mn-TMPyP (**2**, see Fig. 1) was synthesized as described in the Supplementary Information. We used a gp45 E212C mutant of the T4 clamp as a scaffold for conjugation with **2**, because it features a conveniently located cysteine residue on each of the protein monomer subunits, which can be reacted with the maleimide moiety of **2**. The porphyrin catalyst needs to have sufficient flexibility to bind to the minor groove of DNA. To achieve this, the porphyrin moiety was separated from the gp45 clamp by a short water-soluble ethylene glycol segment. The labelling of the gp45 mutant with **2** was carried out with an excess (10 equiv.) of the latter compound for five hours. Owing to the trimeric nature of the clamp and the

[1]Institute for Molecules and Materials, Radboud University Nijmegen, Heyendaalseweg 135, 6525 AJ, Nijmegen, The Netherlands, [2]Education Institute for Molecular Sciences, Radboud University Nijmegen, Heyendaalseweg 135, 6525 ED, Nijmegen, The Netherlands, [3]Department of Chemistry, 801 Chevron Science Center, 219 Parkman Avenue, Pittsburgh, Pennsylvania 15260, USA, [4]Biochemistry, Biophysics & Molecular Biology, Iowa State University, Ames, Indiana 50011, USA, [5]Department of Chemistry, Wartik Laboratory, The Pennsylvania State University, University Park, Pennsylvania 16802, USA; [†]These authors contributed equally to this report. *e-mail: R.Nolte@science.ru.nl; A.Rowan@science.ru.nl

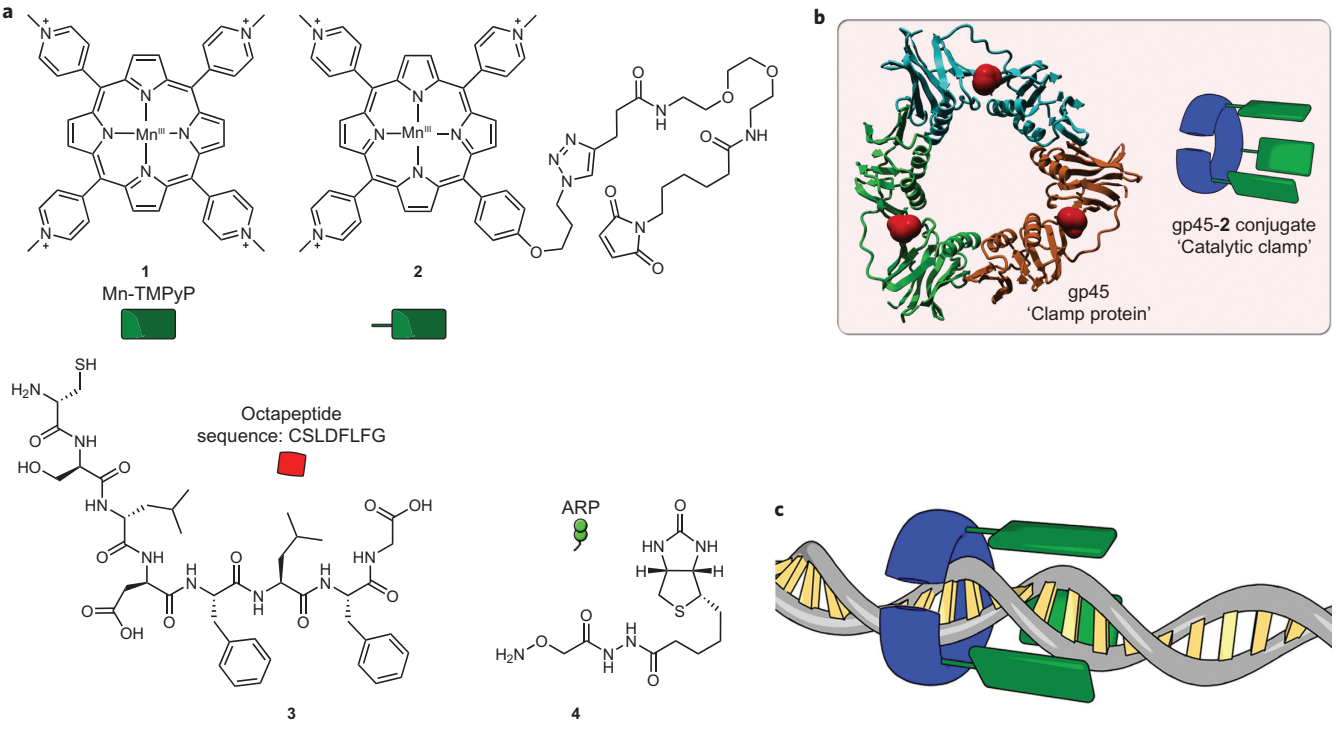

Figure 1 | Molecular structures and schematic representation of the concept for a catalytic clamp. a, Structural formulae, colloquial names and shape representations of small molecules. **b**, Shape representations and colloquial names of proteins and protein conjugates. The E212C mutant of gp45 is shown, and its cysteine residues are emphasized in red. Its structure is based on PDB-file 1CZD with the E212C mutation performed *in silico*. **c**, The concept for a clamp-shaped biohybrid catalyst is based on synthetic catalyst **2**, which is conjugated to the gp45 clamp protein to form a catalytic clamp. This biohybrid catalyst can associate with DNA and slide along it, which confers processivity to the catalytic behaviour of **2**.

presence of a single available cysteine group on each subunit, the resulting gp45–**2** conjugate can contain up to three porphyrin catalysts. Anion-exchange chromatography allowed for the separation of the different compounds containing 1, 2 or 3 porphyrins per trimer. The species with the highest porphyrin content was used for experiments described in this report, and will hereafter be called a 'catalytic clamp'.

Additionally, we synthesized an octapeptide (**3**, Fig. 1) with a sequence similar to the C-terminus of the T4 polymerase (gp43)[20]. This peptide simulates the effect of gp43, leading to clamp-loader departure and effective closure of the gp45 clamp on DNA. Alternatively, the peptide may complete the ring structure of the clamp by binding in the open subunit interface and thus block access by the clamp loader and prevent association of the clamp with DNA substrates.

Interaction of the clamp protein with DNA. Two methods exist to allow gp45 to associate with DNA: it can either be assembled onto DNA via nonspecific binding, or it can be loaded by a specific T4 clamp-loader protein complex (gp44/62)[21,22]. Both techniques have been used to load the clamp successfully onto various DNA substrates. The latter requires the hydrolysis of adenosine triphosphate (ATP) and a suitable DNA template that contains a primer–template site. This gp44/62-mediated loading process can be monitored using an enzyme-coupled adenosine triphosphatase assay[20]. We used this assay to investigate the interaction between octapeptide **3** and the clamp protein. Using a small forked DNA substrate[22], we found that the ATP hydrolysis rate decreased when the octapeptide was titrated into a solution that contained the DNA, gp45 and the clamp–loader complex (see Supplementary Fig. S7). This indicates that less-successful loading events take place, which suggests the alternative explanation above, in which the peptide inhibits clamp loading, applies.

AFM as a tool for detecting the oxidation of DNA. We performed oxidation experiments with the labelled clamp on supercoiled DNA plasmid substrates that consisted of 3,540 base pairs based on a commercially available plasmid (pGEM, see Supplementary Information). The supercoiled form of the plasmid (Form I) provides a sensitive method to probe for oxidation events: introduction of a single-stranded break resulted in uncoiling of the plasmid to the relaxed circular form (Form II)[23]. This transition is monitored easily by conventional agarose gel electrophoresis, owing to the large difference in relative mobility of the two species. Further oxidation events only result in a difference in mobility when a double-stranded break occurs and the plasmid is converted into the linear form (Form III), which requires two oxidation events on opposite strands that are no more than 16 nucleotides apart[24], which is a rare occurrence because of the sequence specificity of our catalyst. Consequently, gel electrophoresis is not a suitable technique if detailed analysis of plasmid oxidations is needed. Furthermore, if nicked DNA is used as starting material, gel electrophoresis cannot detect any oxidations that do not lead to a double-strand break.

As we required a more sensitive oxidation assay, we looked into alternative ways of analysing the reaction products. The group of Meunier has shown that the aldehydes in porphyrin-oxidized DNA oligonucleotides are available for chemical modifications such as reductive amination[25]. An aldehyde-reactive probe (ARP, **4**, Fig. 1) based on hydroxylamine-derived biotin was used to allow a more detailed investigation of the oxidized sites. Through the interaction between biotin and streptavidin, oxidized sites in the plasmid can be marked by a protein, which is a large structural feature compared to the DNA strand (streptavidin has a molecular weight of ~60 kDa and an apparent height of ~4.4 nm, as compared to a typical height of ~1.2 nm for dsDNA). AFM can be used to identify these protein labels[26]. Here, we identify

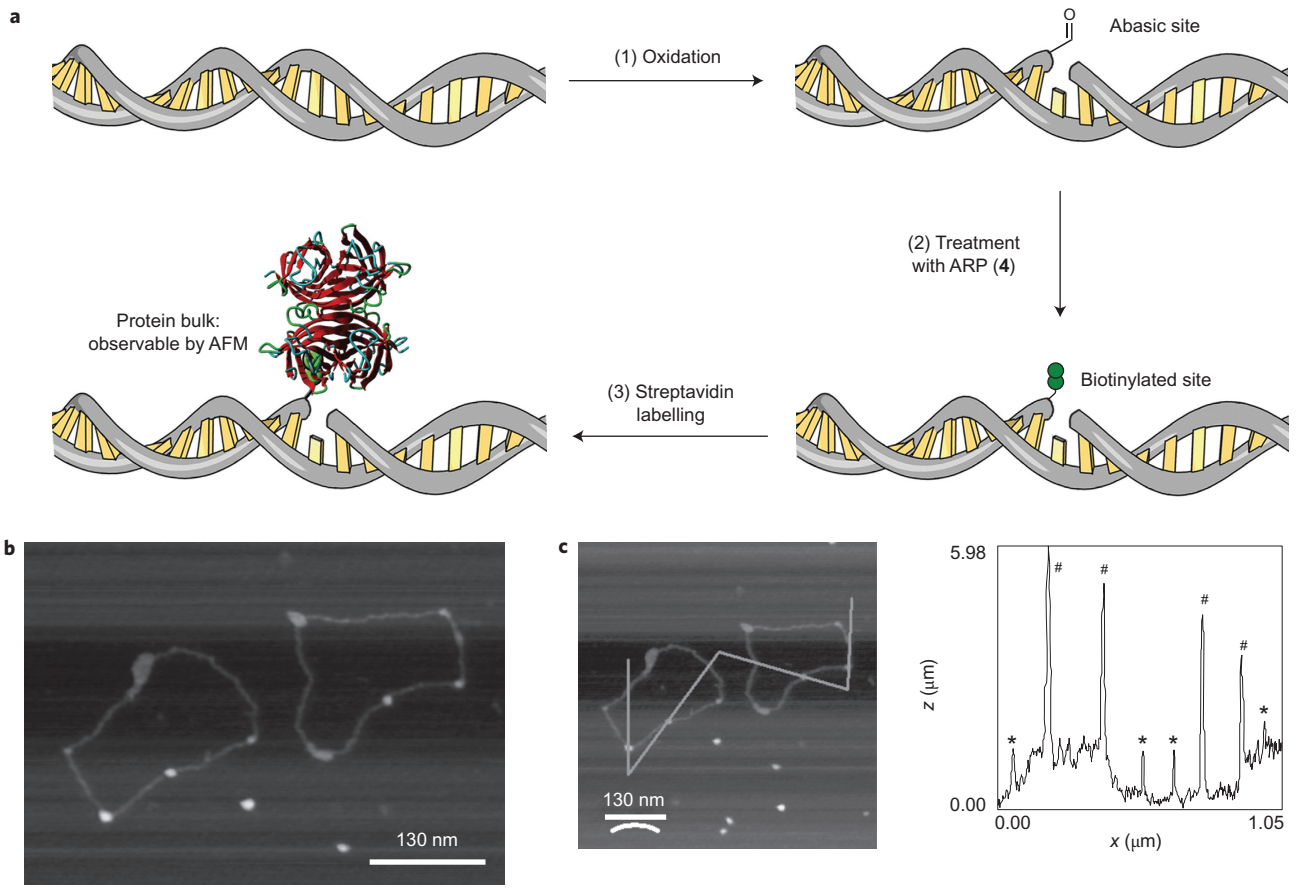

Figure 2 | AFM-based method for detecting DNA oxidation. a, Schematic representation of the detection strategy: (1) DNA oxidation produces an aldehyde, (2) the aldehyde reacts with the ARP reagent **4** to produce a biotinylated site, (3) treatment with streptavidin results in a large object that is connected to the oxidation site, which can be detected by AFM. **b**, Typical AFM height image showing two relaxed circular DNA plasmids with a number of globular features. **c**, Profile analysis along the indicated line in the left panel. Different features are indicated as being a naked DNA strand (*) of typical height 1.2 nm or a DNA strand with a globular feature (#). Streptavidin has an apparent height of ~4.4 nm (3.3–5.4 nm), which corresponds to the height of the globular features labelled by a hatch sign.

streptavidin to determine the number of oxidation events and to elucidate their spatial distribution. A schematic representation of this strategy is presented in Fig. 2a. In the fast-growing body of literature that describes DNA oxidation by porphyrins, the aldehydes have not been used for the quantization of oxidation damage. Moreover, information regarding the spatial distribution of the reactions, to detect processivity in substrate oxidation, could hitherto not be obtained because a suitable assay was not available.

To validate this technique, we incubated DNA with Mn-TMPyP **1** in the presence of $KHSO_5$ as an oxygen donor. After one minute, the reaction was quenched and ARP was added to biotinylate any oxidized sites. The purified solution was supplemented with a streptavidin solution to achieve protein labelling of reaction sites, after which it was analysed by AFM. Figure 2b shows a representative AFM height image that displays two relaxed circular DNA strands with a number of globular features. A profile analysis of this image is given in Fig. 2c. The globular features have apparent heights that range from 3.3 to 5.4 nm, which is in agreement with the height measured for streptavidin (~4.4 nm). This experiment demonstrated that the combination of ARP, streptavidin and AFM provides an alternative tool for assaying DNA oxidation by Mn-porphyrins such as **1**.

Influence of the octapeptide on the catalytic clamp. Supercoiled DNA plasmid was incubated with the catalytic clamp and $KHSO_5$ as an oxygen donor, with or without octapeptide **3** present. Gel electrophoresis confirmed that nearly all supercoiled DNA was converted into the nicked form (see Fig. 3a). As expected, the addition of peptide resulted in a decrease in oxidation efficiency: the binding of the clamp protein to DNA is inhibited by the binding of the peptide to the open subunit interface of a clamp trimer. This suggests that the peptide acts like a switch, reminiscent of the peptide switch in the *Escherichia coli* replication mechanism that mediates processivity by regulating polymerase association with DNA[6]. Plasmids treated with the incubation mixture for one minute were analysed by AFM, and the number of oxidation events per plasmid was recorded for conditions with or without the octapeptide present. Without the peptide, $80 \pm 5\%$ of the plasmids were found to be oxidized in this time span. Oxidized plasmids were observed to have an average of 2.3 bound streptavidin molecules. The histogram shown in Fig. 3b appears to consist of two Poissonian curves with maxima at one or five oxidation events per plasmid. Individual analysis of plasmids from the latter subset revealed that bound streptavidin molecules were often found in clusters (see Fig. 3c). If only distributive oxidation had taken place, these streptavidins would have been uniformly randomly distributed over the plasmids. Statistical analysis of the distances between events suggests that there is a clear difference between the threaded and the non-threaded oxidation mechanisms (see Supplementary Information). We did not detect any clustering in experiments when

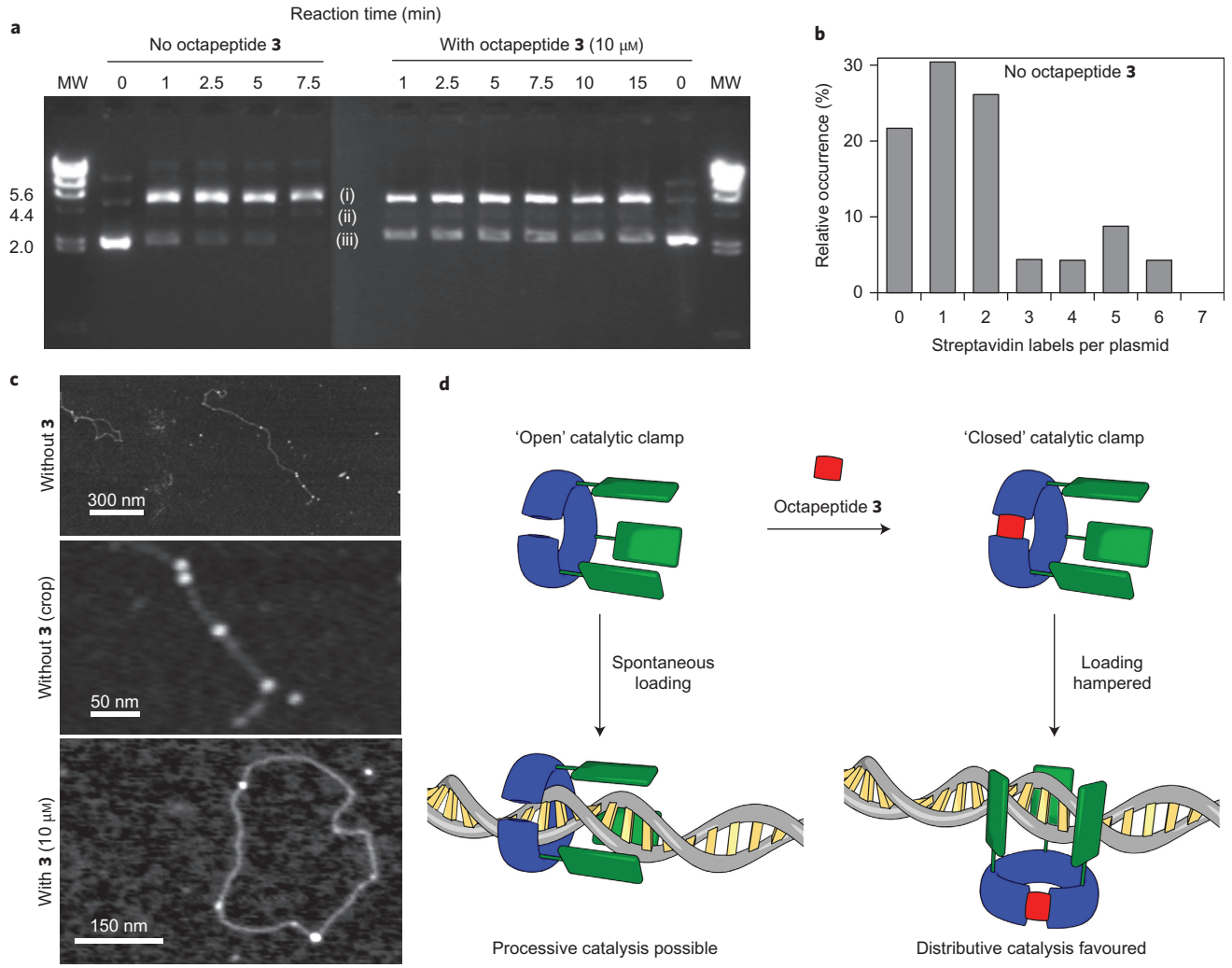

Figure 3 | Octapeptide 3 dictates whether processive or distributive catalysis can take place. a, Experiments in which the supercoiled plasmid were incubated with the catalytic clamp in the presence of $KHSO_5$ (5 μM) with or without octapeptide **3** (10 μM) as indicated. The reaction was stopped after the indicated time (minutes). MW, molecular weight marker (HindIII digest); (i) running height of nicked relaxed plasmids; (ii) running height of linear DNA (faintly visible); (iii) running height of supercoiled plasmids. **b**, Relative frequencies of oxidation reactions on individual plasmids after five minutes based on the streptavidin-labelling analysis. For each encountered plasmid, the number of reactions was counted. No octapeptide was present. **c**, AFM images of plasmids oxidized by the catalytic clamp, with or without octapeptide **3** present, as indicated. Without the peptide, clusters of streptavidin label can be found (top panel and magnified view in the middle panel). These clusters do not appear when the peptide is present (bottom panel). **d**, Schematic representation of the influence of the octapeptide: spontaneous loading of the catalytic clamp can lead to processive oxidation. This is hampered by octapeptide **3**, which closes the open subunit interface of the clamp.

octapeptide **3** was present, and fewer oxidation events took place overall: 55 ± 5% of the plasmids were oxidized, and no more than four streptavidin labels were found on any single plasmid (see Fig. 3c, bottom panel, for a representative plasmid). This reduced catalytic activity suggests that the clamp has a lower affinity for DNA when **3** is present, which corroborates the finding that **3** effectively closes the clamp (Fig. 3d and Supplementary Fig. S7).

The direction of the catalytic clamp can be guided. In nature, the loading of the gp45 clamp protein onto its DNA substrate is mediated by the clamp–loader complex (gp44/62) in an ATP-dependent process[27]. First, the clamp–loader complex associates with the gp45 clamp protein. Subsequently, the clamp is loaded onto DNA at a preferential binding site. These sites can vary from simple nicks in dsDNA to a 5′ extended single overhang[28]. When a nick is used as a loading site, the clamp–loader complex binds to the 3′ end of the nick, and it remains bound as the clamp itself is free to slide over the DNA. Thus, the nick effectively determines the direction in which the clamp will translocate, because one of the two possible paths is physically blocked by the gp44/62 complex (Fig. 4a).

Nicks in plasmids can be created with exact precision by engineered restriction enzymes[29]. Wild-type restriction enzymes are nucleases that recognize and cut fixed DNA sequences, which causes double-stranded breaks. One such restriction enzyme is BbvCI. Its recognition sequence and cut sites are shown in Fig. 4b. Two engineered versions of BbvCI that cut only one of the two strands of the recognition site exist. These two mutants, Nt.BbvCI and Nb.BbvCI, do not cause double-stranded breaks and thus effectively only produce nicks in one of the two strands[29]. Their cut sites are also shown in Fig. 4b. We were interested in whether nicks generated by one of these engineered restriction enzymes could, in effect, create loading sites that, through their predetermined interaction with the clamp–loader complex, specifically direct the catalytic clamp in either the 3′ or the 5′ direction of the plasmid. We selected our

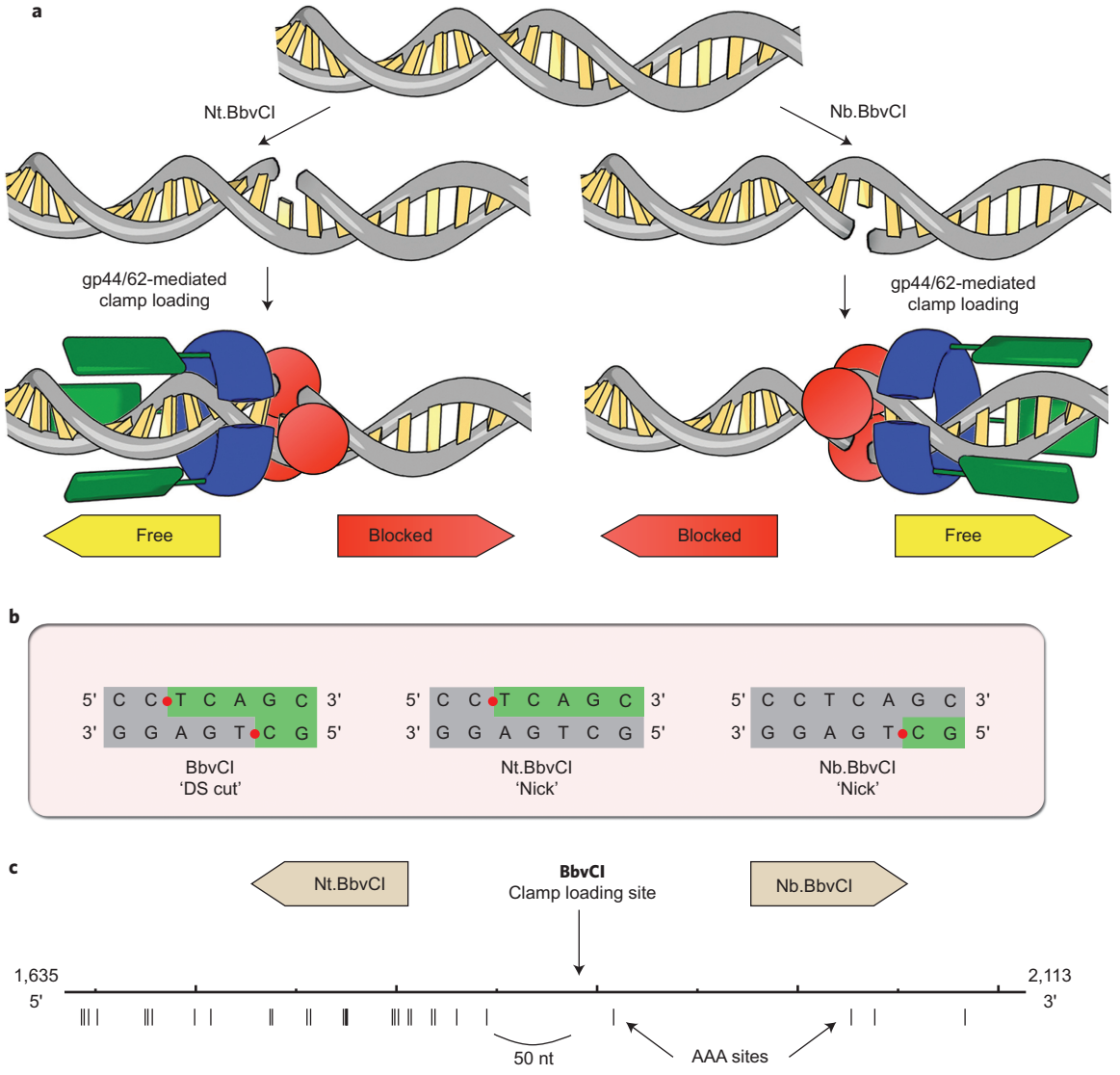

Figure 4 | Guiding the direction of the catalytic clamp. a, Schematic representation of the strategy followed: the clamp-loader complex gp44/62 physically blocks one of the two directions in which the catalytic clamp can slide. When a nick is provided as a loading site, gp44/62 binds to its 3′-end. Therefore, nicks in opposite strands should direct the clamp in opposing directions. **b**, Recognition sequence and cut sites. The restriction endonuclease BbvCI produces sticky ends. Its variants (isoschizomers) Nt.BbvCI and Nb.BbvCI only cut once and thus produce nicks[29]. **c**, Schematic representation showing a segment of the pGEM-derived plasmid (nucleotides (nt) 1,635 to 2,113 from the origin of replication). Potential oxidation sites are marked with black bars below the sequence. The BbvCI restriction site is indicated, and the arrows show the directions that are open to the catalytic clamp when the specified enzymes are used.

pGEM-derived plasmid as the template because, conveniently, it contains only a single recognition site for BbvCI, which lies between two regions that have either low or high AAA-site densities (Fig. 4c). If Nb.BbvCI is used to nick the plasmid, the catalytic clamp should be directed towards a region sparse in potential oxidation sites, whereas a nick caused by Nt.BbvCI should direct the plasmid towards a region with many potential oxidation sites.

To verify this, the plasmid was nicked with either the Nt.BbvCI or the Nb.BbvCI endonuclease, and the catalytic clamp was loaded by the clamp loader. Streptavidin-labelling analysis was successful in identifying oxidation reactions on the nicked substrates. As can be seen in Fig. 5a,b, the different effects of the two BbvCI variants are immediately apparent. When the Nt.BbvCI-nicked substrate was used, the average number of streptavidin molecules per plasmid was 6.1 ± 1.6. For the Nb.BbvCI substrate, this number was significantly lower, namely 1.9 ± 1.2 (see Fig. 5c). This observation correlates with the situation outlined in Fig. 4, in which the clamp is loaded and subsequently migrates towards regions with either a high or a low number of oxidation sites. Moreover, visual inspection of the location of streptavidin labels on Nt.BbvCI-nicked substrates revealed that oxidations consistently occurred in clusters. To reach the first cluster of AAA sites in the 5′ direction of the loading site, the catalytic clamp would have to slide across more than 40 base pairs on the substrate, which clearly demonstrates the processive nature of this hybrid catalyst.

Conclusion

We constructed a novel biohybrid artificial enzyme based on the T4 clamp protein and a conjugated cationic manganese-porphyrin catalyst. The resulting catalytic clamp is capable of translocating along a DNA template and oxidizing AAA sites. To analyse its activity, we developed an AFM-based method in which oxidized sites on the plasmid are labelled with streptavidin. Identification of the streptavidin labels on the DNA substrate by AFM successfully detected

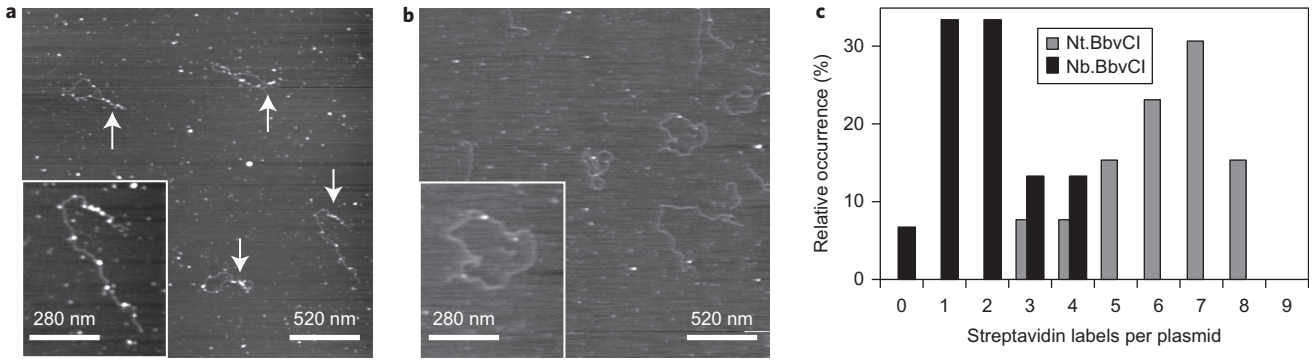

Figure 5 | AFM analysis of plasmids oxidized by a guided catalytic clamp. a, AFM image of streptavidin-labelled plasmids after five minutes of oxidation by the catalytic clamp. The clamp was loaded by the gp44/62 clamp-loader complex on a nick produced by Nt.BbvCI. Arrows point to regions with a row of multiple streptavidin labels. **b**, AFM image of streptavidin-labelled plasmids after oxidation by the catalytic clamp. The clamp was loaded by the gp44/62 clamp-loader complex on a nick produced by Nb.BbvCI. The lack of clustered streptavidin labels is apparent. **c**, Quantification of the amount of oxidation reactions on individual plasmids based on streptavidin-labelling analysis. The relative frequency of the number of streptavidin labels is given for each plasmid. The catalytic clamp was loaded on nicks produced by either Nb.BbvCI or Nt.BbvCI, and a significant difference between the resulting amount of oxidation was found (two-sample *t*-test, $p < 0.0001$).

oxidation events and gathered information about their relative location, which hitherto had not been possible.

Dependent on the reaction conditions, the biohybrid catalyst displayed either distributive or processive catalytic behaviour on DNA substrates. In cases where the protein was bound to DNA through nonspecific binding, clusters of streptavidin labels in close proximity could be observed on the same plasmid, which implies processive catalysis. Such clusters were not found when the catalytic clamp was 'closed' by octapeptide **3**, a structural mimic of the sequence that naturally completes the circular shape of the clamp. In this closed state, the catalytic clamp could not associate with its DNA template and thus all reaction products were the result of distributive actions.

In nature, the T4 clamp protein is loaded onto recognition sites in DNA by a clamp–loader complex (gp44/62). The orientation of the recognition site determines the direction in which the clamp will slide along the DNA template. We could generate enzymatically two mirrored loading sites, guiding the clamp to stretches of DNA that were either rich or poor in potential reaction sites. The unique ability of our AFM method to detect catalytic events allowed us to verify that when this directed enzymatic loading strategy was applied, the catalyst would, indeed, slide towards the chosen region. If the catalytic clamp was guided towards the substrate-rich region, we could detect that many streptavidin labels appeared in clusters. When the clamp slid over the substrate-poor region, a lower total amount of oxidation events was found, and no clusters of two or more labels were detected.

Combined, this report shows that using concepts from nature, such as toroidal mediators, the performance of catalytic reactions may be influenced and guided, which allows the development of more-efficient life-like catalysts for the modification of linear substrates, and eventually synthetic polymers also.

Methods

Oxidation of supercoiled DNA by the catalytic clamp. As shown in Supplementary Fig. S8, various oxygen-donor concentrations were tried. The catalytic clamp, at a concentration of 400 nM, was incubated with supercoiled plasmid (25 ng μl^{-1}) in the presence of 50 $\mu g\ ml^{-1}$ bovine serum albumin (BSA). When indicated, peptide **3** (10 μM) was added. After five minutes, the reaction was started by the addition of $KHSO_5$ to final concentrations of 5, 10 or 20 μM, always taking care to bring the total volume of the reaction to 60 μl. At the indicated times, the reactions were quenched, extracted and analysed by SDS–polyacrylamide gel electrophoresis (see Supplementary Fig. S8) or AFM (see Fig. 3.)

Oxidation of nicked DNA by the catalytic clamp. The catalytic clamp at a concentration of 250 nM was incubated with Nt.BbvCI- or Nb.BbvCI-nicked DNA (25 ng μl^{-1}) in the presence of 50 $\mu g\ ml^{-1}$ BSA, 2 mM ATP and 125 nM gp44/62. After five minutes, the reaction was started by the addition of $KHSO_5$ to a concentration of 20 μM to bring the total volume of the reaction to 25 μl. After five minutes the reactions were quenched, extracted and analysed by AFM as described below, the results of which are shown in Fig. 5.

Biotinylation and AFM-analysis of oxidized plasmids. Quenched samples from oxidation reactions were incubated with 4 mM ARP reagent **4**, biotinylating aldehydes in DNA with a sensitivity down to 2.4 aldehydes per 107 base pairs[30]. After 1.5 hours, the amination reaction was quenched by the addition of a dilute $NaCNBH_3$ solution. The reactions were then incubated for 15 minutes, and the DNA was precipitated in ethanol by the addition of 0.1 volume 3M NaOAc pH 5.3 and 2.5 volumes EtOH, followed by incubation at −20 °C for 30 minutes. Then the solutions were centrifuged at 16,000*g* for 15 minutes, after which the pellets were resuspended in ice-cold EtOH (70%) followed by an additional ten minutes of centrifugation. The pellets were then dried in air and dissolved in AFM buffer (40 mM HEPES pH 7.4, 10 mM $MgCl_2$) and 10 equiv. streptavidin were added per total amount of potential oxidation sites (~190 per plasmid). After the addition of streptavidin, the samples were incubated for another 30 minutes before they were purified from excess streptavidin by a G100 Sephadex column equilibrated in AFM buffer. The fraction with the highest amount of DNA was analysed by AFM. A sample (2 μl) of the first protein-containing fraction was incubated for five minutes on freshly cleaved mica, washed with 1 ml MilliQ water, dried by air flow and analysed by AFM. For Fig. 3b, 23 plasmids were analysed. For Fig. 5c, 13 Nt.BbvCI-nicked plasmids and 15 Nb.BbvCI-nicked plasmids were analysed. Circular plasmids may sometimes break and become linear during sample preparation for AFM analysis; linear plasmids were not necessarily formed by oxidative catalysis.

Received 18 October 2012; accepted 8 August 2013; published online 22 September 2013; corrected online 26 September 2013

References

1. Breyer, W. A. & Matthews, B. W. A structural basis for processivity. *Protein Sci.* **10,** 1699–1711 (2001).
2. Stillman, B. Smart machines at the DNA-replication fork. *Cell* **78,** 725–728 (1994).
3. Kovall, R. & Matthews, B. W. Toroidal structure of λ-exonuclease. *Science* **277,** 1824–1827 (1997).
4. Benkovic, S. J., Valentine, A. M., & Salinas, F. Replisome-mediated DNA replication. *Annu. Rev. Biochem.* **70,** 181–208 (2001).
5. Champoux, J. J. DNA topoisomerases: structure, function, and mechanism. *Annu. Rev. Biochem.* **70,** 369–413 (2001).
6. López de Saro, F. J., Georgescu, R. E. & O'Donnell, M. A peptide switch regulates DNA polymerase processivity. *Proc. Natl Acad. Sci. USA* **100,** 14689–14694 (2003).
7. Indiani, C., McInerney, P., Georgescu, R., Goodman, M. F & O'Donnell, M. A sliding-clamp toolbelt binds high- and low-fidelity DNA polymerases simultaneously. *Mol. Cell* **19,** 805–815 (2005).
8. Trakselis, M. A., Alley, S. C., Abel-Santos, E. & Benkovic, S. J. Creating a dynamic picture of the sliding clamp during T4 DNA polymerase holoenzyme assembly by using fluorescence resonance energy transfer. *Proc. Natl Acad. Sci. USA* **98,** 8368–8375 (2001).

9. Yang, J., Zhuang, Z., Roccasecca, R. M., Trakselis, M. A. & Benkovic, S. J. The dynamic processivity of the T4 DNA polymerase during replication. *Proc. Natl Acad. Sci. USA* **101,** 8289–8294 (2004).
10. Breslow, R. Artificial enzymes. *Science* **218,** 532–537 (1982).
11. Murakami, Y., Kikuchi, J., Hisaeda, Y. & Hayashida, O. Artificial enzymes. *Chem. Rev.* **96,** 721–758 (1996).
12. Nanda, V. & Koder, R. L. Designing artificial enzymes by intuition and computation. *Nature Chem.* **2,** 15–24 (2010).
13. Takashima, Y., Osaki, M., Ishimaru, Y., Yamaguchi, H. & Harada, A. Artificial molecular clamp: a novel device for synthetic polymerases. *Angew. Chem. Int. Ed.* **50,** 7524–7528 (2011).
14. Thordarson, P., Bijsterveld, E. J., Rowan, A. E. & Nolte, R. J. Epoxidation of polybutadiene by a topologically linked catalyst. *Nature* **424,** 915–918 (2003).
15. Coumans, R. G. E., Elemans, J., Nolte, R. J. M. & Rowan, A. E. Processive enzyme mimic: kinetics and thermodynamics of the threading and sliding process. *Proc. Natl Acad. Sci. USA* **103,** 19647–19651 (2006).
16. Monnereau, C. *et al.* Porphyrin macrocyclic catalysts for the processive oxidation of polymer substrates. *J. Am. Chem. Soc.* **132,** 1529–1531 (2010).
17. Meunier, B. Metalloporphyrins as versatile catalysts for oxidation reactions and oxidative DNA cleavage. *Chem. Rev.* **92,** 1411–1456 (1992).
18. Pratviel, G., Bernadou, J. & Meunier, B. DNA and RNA cleavage by metal complexes. *Adv. Inorg. Chem.* **45,** 251–312 (1998).
19. Bernadou, J. & Meunier, B. Biomimetic chemical catalysts in the oxidative activation of drugs. *Adv. Synth. Catal.* **346,** 171–184 (2004).
20. Berdis, A., Soumillion, P. & Benkovic, S. The carboxyl terminus of the bacteriophage T4 DNA polymerase is required for holoenzyme complex formation. *Proc. Natl Acad. Sci. USA* **93,** 12822–12827 (1996).
21. Zhuang, Z. H., Berdis, A. J. & Benkovic, S. J. An alternative clamp loading pathway via the T4 clamp loader gp44/62–DNA complex. *Biochemistry* **45,** 7976–7989 (2006).
22. Smiley, R. D., Zhuang, Z. H., Benkovic, S. J. & Hammes, G. G. Single-molecule investigation of the T4 bacteriophage DNA polymerase holoenzyme: multiple pathways of holoenzyme formation. **45,** 7990–7997 (2006).
23. Vologodskii, A. V., Lukashin, A. V., Anshelevich, V. V. & Frank-Kamenetskii, M. D. Fluctuations in superhelical DNA. *Nucleic Acids Res.* **6,** 967–982 (1979).
24. Freifeld, D. & Trumbo, B. Matching of single-strand breaks to form double-strand breaks in DNA. *Biopolymers* **7,** 681–693 (1969).
25. Pratviel, G., Duarte, V., Bernadou, J. & Meunier, B. Nonenzymic cleavage and ligation of DNA at a three A•T base pair site. A two-step pseudohydrolysis of DNA. *J. Am. Chem. Soc.* **115,** 7939–7943 (1993).
26. Neish, C. S., Martin, I. L., Henderson, R. M. & Edwardson, J. M. Direct visualization of ligand–protein interactions using atomic force microscopy. *Br. J. Pharmacol.* **135,** 1943–1950 (2002).
27. Alley, S. C., Abel-Santos, E. & Benkovic, S. J. Tracking sliding clamp opening and closing during bacteriophage T4 DNA polymerase holoenzyme assembly. *Biochemistry* **39,** 3076–3090 (2000).
28. Jarvis, T. C., Paul, L. S., Hockensmith, J. W. & Von Hippel, P. H. Structural and enzymatic studies of the T4 DNA replication system. II. ATPase properties of the polymerase accessory protein complex. *J. Biol. Chem.* **264,** 12717–12729 (1989).
29. Heiter, D. F., Lunnen, K. D. & Wilson, G. G. Site-specific DNA-nicking mutants of the heterodimeric restriction endonuclease R.BbvCI. *J. Mol. Biol.* **348,** 631–640 (2005).
30. Nakamura, J. *et al.* Highly sensitive apurinic/apyrimidinic site assay can detect spontaneous and chemically induced depurination under physiological conditions. *Cancer Res.* **58,** 222–225 (1998).

Acknowledgements

We thank M. M. Spiering and Z. Zhuang for their assistance and for useful discussions. We thank M. B. Castells and D. van de Mosselaar for synthetic assistance. This work was supported by the Royal Netherlands Academy of Arts and Sciences (R.J.M.N.), NWO Vici (A.E.R.), a research grant from the European Research Council (ERC-2011-AdG 290886 ALPROS to S.F.M.v.D. and R.J.M.N.) and finance from the Dutch Ministry of Education, Culture and Science (Gravity program 024.001.035).

Author contributions

S.J.B. and R.J.M.N. conceived the experiments and A.E.R., R.J.M.N., S.F.M.v.D. and J.C. designed the experiments. J.C. performed the experimental work and was supervised by J.J.L.M.C. K.N. developed the AFM-analysis. M.A.T. and S.W.N. provided expertise on protein design and expression. T.G.B. performed statistical analysis. S.F.M.v.D. performed additional experimental work. J.C., S.F.M.v.D., K.N., T.G.B., A.E.R. and R.J.M.N. analysed and interpreted the results. S.F.M.v.D. and J.C. co-wrote the manuscript and S.J.B., A.E.R., R.J.M.N., K.N., M.A.T., S.W.N. and T.G.B. commented on it.

Additional information

Supplementary information is available in the online version of the paper. Reprints and permissions information is available online at www.nature.com/reprints. Correspondence and requests for materials should be addressed to A.E.R. and R.J.M.N.

Competing financial interests

The authors declare no competing financial interests.